NAVAL SHIP RESEARCH AND DEVELOPMENT CENTER
Washington, D.C. 20007

FLUTTER OF A TWO-DEGREE-OF-FREEDOM HYDROFOIL IN TWO-DIMENSIONAL SUBCAVITATING FLOW

by
Daniel S. Cieslowski and
Peter K. Besch

DEPARTMENT OF HYDROMECHANICS
RESEARCH AND DEVELOPMENT REPORT

January 1970 Report 3163

The Naval Ship Research and Development Center is a U.S. Navy center for laboratory effort directed at achieving improved sea and air vehicles. It was formed in March 1967 by merging the David Taylor Model Basin at Carderock, Maryland and the Marine Engineering Laboratory at Annapolis, Maryland. The Mine Defense Laboratory, Panama City, Florida became part of the Center in November 1967.

Naval Ship Research and Development Center
Washington, D.C. 20007

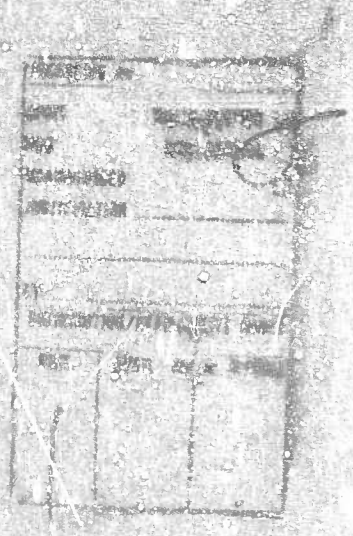

DEPARTMENT OF THE NAVY
NAVAL SHIP RESEARCH AND DEVELOPMENT CENTER
WASHINGTON, D. C. 20007

FLUTTER OF A TWO-DEGREE-OF-FREEDOM HYDROFOIL IN TWO-DIMENSIONAL SUBCAVITATING FLOW

by

Daniel S. Cieslowsi and
Peter K. Besch

January 1970 Report 3183

TABLE OF CONTENTS

LIST OF FIGURES

LIST OF TABLES

NOTATION

Symbol	Definition
a	Distance of pitch axis from midchord of hydrofoil model, in units of semichord (positive aft)
b	Semichord of hydrofoil model
f	Flutter frequency in hertz
f_h	Natural frequency of uncoupled heave oscillation in air; theoretically $\sqrt{k_h/(m_h + m_\alpha)}$
f_α	Natural frequency of uncoupled pitch oscillation in air; theoretically $\sqrt{K_\alpha/I_\alpha}$
h	Vertical displacement of pitch axis from equilibrium position (positive downward)
I_α	Second moment of inertia of rotating mass about pitch axis
K_h	Heave spring stiffness
K_α	Pitch spring stiffness
L	Lift, positive upward
M	Pitching moment, positive when acting to increase angle of attack
m_h	Mass of hydrofoil model and suspension which only translates
m_α	Mass of hydrofoil model and suspension which both rotates and translates
P_v	Water vapor pressure
P_∞	Static pressure
r_α	Radius of gyration of rotating mass, in units of semichord; $\sqrt{I_\alpha/m_\alpha}\ /b$
S_α	First moment of inertia of rotating mass about pitch axis
s	Span of hydrofoil model
U	Free stream velocity
x_α	Distance of center of gravity from pitch axis, in units of semichord (positive aft); $S_\alpha/m_\alpha b$
α	Angle of attack of hydrofoil model; refers to rotational mode when used as a subscript
β	Ratio of rotating mass to total mass of system; $m_\alpha/(m_h + m_\alpha)$
θ	Mean angle of attack
θ_0	Zero-speed angle of attack
μ	Mass ratio of system; $(m_\alpha + m_h)/\pi\rho b^2 s$

ρ	Mass of water per unit volume
σ_v	Cavitation number based on water vapor pressure; $2(p_\infty - p_v)/\rho U^2$
ω	$2\pi f$
ω_h	$2\pi f_h$
ω_α	$2\pi f_\alpha$

ABSTRACT

Four hydrofoil flutter tests were performed in the towing basin and the 36-inch water tunnel at the Naval Ship Research and Development Center using a two-degree-of-freedom hydrofoil in two-dimensional flow. Mass ratio, mass unbalance, heave stiffness, angle of attack, and foil depth were varied. All of these parameters significantly affected the flutter boundaries.

Comparisons were made with a flutter theory based on the Theodorsen analysis. Theory gave good flutter predictions at high mass ratios but failed at low mass ratios.

ADMINISTRATIVE INFORMATION

This work was funded under the Hydrofoil Development Program of the Naval Ship Systems Command, Subproject S4606, Task 1703.

INTRODUCTION

Flutter is defined as a negatively damped oscillation of a winglike structure which is coupled to a surrounding fluid. Since the oscillation would increase in amplitude until structural failure occurred unless other limiting factors were present, flutter must be avoided in practice. It is well known that flutter can occur on airplane wings and control surfaces that are improperly designed. Within the last several years, flutter has been demonstrated on hydrofoil models by a number of experimenters.[1-4] Although flutter has not occurred on a full-scale hydrofoil craft, it is a potential danger to future hydrofoil craft and other vessels having struts and control surfaces, including conventional ships.

The problem of flutter in the aerodynamic regime has been successfully treated by the representative section theory developed by Theodorsen.[5] When applied to hydrofoil flutter, however, representative section theory fails in an unconservative manner in the low mass ratio region of practical interest, according to Reference 3 and an unpublished calculation by the authors for the hydrofoil of Reference 4. Flutter theories of greater

---

[1]References are listed on page 35.

sophistication than representative section theory also exhibit deficiencies in the hydrodynamic regime.[6] For example, Rowe[7] performed a flutter calculation in which he carried out an evaluation of the structural representation of the flutter models. His conclusion was that the hydrodynamic load theory rather than the structural theory was at fault.

Henry[8] carried out a series of flutter tests in which both the structural and the hydrodynamic aspects of the experimental configuration were simplified. A fully wetted hydrofoil was placed in a test section which produced two-dimensional flow. Only two degrees of freedom were permitted; pitch and heave. This configuration simulated an ideal representative section of the type mentioned above. As in other cases, the Henry results showed that the Theodorsen theory was conservative at high mass ratios approximating the aerodynamic regime, but unconservative at low mass ratios. In view of the structural simplicity of the experimental system, these results appear to confirm that hydrodynamic aspects of the theory are at fault. Since two-dimensional flow was at least approximated in this experiment, the deficiencies in the Theodorsen theory were probably inherent in the treatment of two-dimensional flow rather than in the neglect of three-dimensional flow effects.

The present work was carried out to obtain additional data of the type Henry obtained, but for a number of different parameter ranges. A two-degree-of-freedom hydrofoil system was tested in two-dimensional, noncavitating flow in a water tunnel and in a towing basin. Heave stiffness, angle of attack, and foil depth were varied in addition to the mass ratio and mass unbalance variations studied by Henry. However, none of the present data are directly comparable to the Henry data because other parameters were different.

The experimental results reported were obtained from four series of flutter tests conducted during 1964, 1965, and 1966. Data obtained from the 1964 tests were reported in Reference 9, but comparisons between theory and experiment in that reference are incorrect because a number of parameters were normalized improperly. The 1966 tests also included flutter testing of a cavitating hydrofoil, the results of which have been reported in Reference 6.

EXPERIMENTAL EQUIPMENT

TEST FACILITIES

Three series of flutter tests were performed in the NSRDC high-speed towing basin.[10] The basin is 2966 ft long and 21 ft wide; it is 10 ft deep for 1168 ft of its length and 16 ft deep for the remaining 1800 ft. All experimental apparatus was mounted on a high-speed towing carriage (Carriage 5) which has a maximum speed of 60 knots.

One series of flutter tests was performed in the NSRDC 36-in. variable-pressure water tunnel.[10] The tunnel is a closed-circuit system for which both open- and closed-jet test sections are available. The open-jet test section was used for the flutter tests. The maximum speed through the test section is 50 knots. Static pressure at the test section centerline can be varied from 4 to 60 psia.

TWO-DIMENSIONAL TEST SECTION

Large parallel end plates 21 in. apart were used in both test facilities to produce two-dimensional flow past the hydrofoil which was mounted 18.5 in. above the bottom of the end plates. The end plates were 37.5 in. high and had sharp leading edges. Faired boxes on the outside of the end plates contained the foil suspensions.

End plates of two different lengths were used; 40-in. end plates were the longest that would fit in the test section of the 36-in. water tunnel. The end plates were lengthened to 58 in. for testing in the towing basin so that the foil suspension boxes on the outside of the end plates would lie within the Kelvin wave envelope emanating from the leading edge of the end plate, resulting in minimum flow blockage. The test section is illustrated in Figure 1.

The end plates were held by a superstructure which was attached to the test facility by a suitable bracket. In the 36-in. water tunnel, the end plates were mounted vertically in the open-jet test section and were completely submerged during testing. There was no free surface in the water tunnel test section. In the towing basin, they were suspended vertically below the high-speed towing carriage in a surface-piercing configuration. Sliding attachments permitted the hydrofoil to be operated at

several water depths. In addition to the superstructure bracings, it was found necessary in both facilities to connect the bottom part of the end plates with three faired braces to maintain the separation distance against forces caused by the effective camber of the end plate-box combination. Water speeds were limited to approximately 30 knots because of the large drag force. Tunnel blockage further limited speeds in the water tunnel to approximately 25 knots.

NACA 16-209 HYDROFOIL MODEL

The hydrofoil test model was constructed of solid titanium with dimensions as shown in Figure 2. The NACA 16-209 profile was chosen so that the hydrofoil would remain free of cavitation at all test conditions. The minimum cavitation number expected was $\sigma_v = 0.83$, which corresponds to the maximum speed of 30 knots and the minimum depth of 3.5 in. According to a pressure distribution obtained from potential flow analysis,[11] the cavitation inception number of the test hydrofoil at 0 deg incidence was expected to be 0.32. Experimental results[12] have indicated that the inception σ_v should be approximately doubled at a 3-deg angle of attack. Cavitation inception was obtained at $\sigma_v = 0.54$ in the 36-in. water tunnel for this condition. Therefore, cavitation was not expected to occur in the towing basin tests.

TWO-DEGREE-OF-FREEDOM FOIL SUSPENSION

A system of flexures was used to limit foil motion to two degrees of freedom: the heave mode, which is translation normal to the flow, and the pitch mode. The mechanism is shown schematically in Figure 3. Each end of the hydrofoil was held by an inner housing which could rotate relative to an outer housing with a torsional stiffness determined by the pitch flexures. Heave stiffness was governed by large coil springs at each end (two springs were used, one inside the other) in addition to the heave flexures. The heave flexures secured the housings against drag and prevented rotation of the outer housing. The suspensions were installed on the outside of parallel test section walls, with the foil mounting bosses extending through a circular hole in each wall to the suspensions.

The foil was centered in the wall openings at all run velocities by adjusting the coil spring compression to cancel the steady component of the lift. The wall openings acted as mechanical stops to heave motion, allowing the foil an amplitude of ± 1/2 in. Pitch motion was limited to ± 8 deg by pins in the housing assemblies. The foil angle of attack was controlled by a worm gear within each inner housing and could be varied over 360 deg.

The foil suspension may be characterized by the structural parameters shown in Figure 4. The hydrofoil rotates about its pitch axis, which is located a distance ab aft of midchord, where b is the length of the semichord. For this type of suspension, a is determined by the hydrofoil model; the hydrofoil model used in the present experiments had a = -0.4, which is equivalent to a pitch axis located 30 percent of the chord aft of the leading edge. The center of gravity of all rotating components is located x_α semichords aft of the pitch axis. x_α, called the mass unbalance, is continuously and independently varied by rotating two pairs of eccentric weights about shafts attached to the inner housings on the pitch axis. The four eccentric weights, two concentric weights, the inner housings, and the foil itself determine the rotating mass m_α and the radius of gyration r_α. The nonrotating mass m_h consists of the outer housing mass plus one third the mass of the coil springs. The rotational spring constant K_α is determined by the pitch flexures, and the translational spring constant K_h is determined by the coil springs and the heave flexures.

Two mass ratios μ and β were used in the flutter analysis. The mass ratio μ is defined as the ratio of the total mass to the mass of a cylinder of water circumscribing the foil or

$$\mu = (m_h + m_\alpha) / \pi\rho b^2 s$$

The ratio of the rotating mass to the total mass is

$$\beta = m_\alpha / (m_h + m_\alpha)$$

Experimental values of the structural parameters are given in Table 1. Spring constants K_h and K_α were obtained by static applications of forces and moments to the hydrofoil. The mass unbalance x_α and radius of gyration r_α were obtained from measurements of the first and second

moments of inertia S_α and I_α of the rotating masses about the pitch axis, respectively. The first moments of inertia S_α were determined by combining the first moments of the individual eccentric weights and the hydrofoil. The second moments of inertia I_α were calculated from the measured in-air natural frequencies of the rotating system. These values were corrected for the experimentally determined added mass and moment of the suspensions but not of the foil. The structural parameter values given in Table 1 therefore approximate the in-vacuum characteristics of the hydrofoil system needed for theoretical analysis.

The above-described foil suspension design placed certain limitations on the variation of structural parameters. Only x_α and α could be changed independently of all other parameters. Changes in μ, accomplished by changing the eccentric weights, produced changes in r_α, β, f_h, and f_α. Similarly, changes in K_h, produced by using different coil springs, affected μ, β, f_h, and f_α. Since several parameters were thus linked to mass ratio, it was found convenient to specify structural configurations in terms of mass ratio μ, mass unbalance x_α, zero-speed angle of attack θ_o, and foil depth. A complete list of the other parameter values for each value of μ tested is given in Table 1.

EQUATIONS OF MOTION

The equations of motion for the coupled, two-degree-of-freedom hydrofoil system in two-dimensional flow are as follows:

$$\begin{aligned} (m_h + m_\alpha)\,\ddot{h} + S_\alpha\,\ddot{\alpha} + K_h\,h &= -L \\ I_\alpha\,\ddot{\alpha} + S_\alpha\,\ddot{h} + K_\alpha\,\alpha &= M \end{aligned} \qquad [1]$$

where the dots indicate differentiation with respect to time. The hydrodynamic lift L and moment M are functions of the pitch and heave coordinates and the flow parameters. Flutter characteristics are obtained by determining the flow parameters which satisfy Equation [1] for simple harmonic motion, which corresponds to zero damping.

INSTRUMENTATION

Foil motion was monitored by pen recordings of the output of strain gages attached to the pitch and heave flexures.

Carriage speeds in the high-speed towing basin were determined by reference to digital printouts generated by the carriage control system at the rate of two per second.

Water speed and tunnel pressure in the 36-in. variable-pressure water tunnel were determined by pressure taps built into the tunnel. Automatic readouts for these quantities were provided.

During the final series of tests, conducted in 1966, several still photographs and one motion picture film were taken of the hydrofoil. No other photography was used.

PROCEDURE

The flutter tests were performed in four series over a period of 3 years. Each series was designed to vary a number of parameters. In the first series, conducted in the 36-in. variable-pressure water tunnel during October 1964, mass ratio μ and mass unbalance x_α were varied. In the second series, conducted in the high-speed towing basin also during October 1964, the same values of μ and x_α were used in order to provide a comparison between the two facilities. The third series, conducted in the towing basin during June and July of 1965, tested several foil depths and angles of attack in addition to varying μ and x_α. In the fourth series, conducted in the towing basin during July and August of 1966, μ was varied in such a manner that a large range of heave frequency f_h was tested in addition to varying x_α. The fourth series also included flutter testing of a cavitating hydrofoil which has been previously reported.[6]

In order to obtain flutter of the hydrofoil in the water tunnel, the water speed was gradually increased until regular foil oscillations of small amplitude occurred. Slightly higher speeds caused the oscillations to grow in amplitude. The flutter boundary was considered to have been passed when the oscillation amplitude became large compared to ambient random fluctuations; no quantitative criterion was established. Because of the blockage effect of the flutter apparatus in the water tunnel test section, water speeds were limited to approximately 25 knots.

Flutter speed boundaries in the towing basin were determined by towing the foil at several speeds on successive runs until relatively large foil oscillations occurred. In most cases, additional runs were made to define the critical flutter speeds more precisely, but no quantitative criterion was used to identify flutter. Flutter speeds were taken from nonaccelerating portions of the runs.

FLUTTER RESULTS

Flutter boundaries determined in the four series of tests are given in Tables 2 through 6. The boundaries consist of flutter inception speeds, flutter frequencies, and relative phase angles between pitch and heave motion during flutter. Maximum test speeds for parameter values at which flutter did not occur are also given. No attempt was made to determine amplitude ratios. Some of the flutter data are plotted in reduced form as functions of mass unbalance x_α or frequency ratio ω_h/ω_α in Figures 5 through 21 for the purpose of determining parametric effects. Flutter-free speed ranges have been indicated by vertical lines when flutter did not occur. Theoretically predicted flutter boundaries are also plotted and will be discussed below.

Flutter boundaries were affected by several sources of experimental uncertainty. No precise method of determining the flutter boundary was available for either water-tunnel or towing-basin tests, because the oscillations that occurred did not grow continuously until limited by the mechanical stops. Instead, the oscillations were self-limited to amplitudes well within the mechanical stops at speeds near oscillation inception. The amplitudes increased with speed but did not reach the stops. Flutter was considered to have occurred when the oscillations became large compared to ambient flow noise. Another source of experimental uncertainty was the fact that the number of test runs was limited, and so in some cases, speed increments were not as small as desired. In addition the zero-speed angle of attack θ_o varied up to 0.25 deg from the nominal values given in Tables 2 through 5 as a result of changes in the static moment in changing x_α. During testing, the mean angle of attack θ increased by about 0.1 deg at maximum speeds because of the hydrodynamic pitching moment.

Two additional effects were present which might have distorted the flutter boundaries. First, pre-run acceleration was very small in the water tunnel and much larger in the towing basin. Furthermore, carriage runs made in 1964 and 1965 approached run speed during acceleration while runs made in 1966 approached run speed during deceleration following a 5 percent speed overshoot. Oscillograph records from a typical flutter run made in 1966 are shown in Figure 22, along with the carriage speed curve. A comparison of different series of runs indicated that acceleration did not affect the flutter boundaries. The second effect was cavitation. Although the NACA 16-209 hydrofoil was not expected to cavitate, cavitation was observed along the leading edge of the foil in photographs made at speeds of 28 knots and above in the towing basin during the 1966 test series. Such conditions correspond to a cavitation number of 0.96. The cavities reached a maximum of 0.2 chords in length at the midspan of the foil and decreased to zero length at the ends of the foil. Although cavitation may have occurred during the earlier tests, no flow observations were made.

Flutter results obtained in the two different test facilities are compared in Figures 5 through 7. Note that the flutter speeds obtained in the water tunnel were slightly lower than those obtained at a 7-in. depth in the towing basin. The difference increased with increasing x_α. Flutter frequencies were also lower in the water tunnel but became equal to towing basin frequencies at high x_α. Phase angle differences showed no definite trend. Since both foil depth and pre-run acceleration differed between the two test series, it is not possible to say which effect was responsible for the deviations. However, since the maximum deviation in flutter speed was only 5 percent, which is comparable to the experimental uncertainty, the two effects were either mutually cancelling or both quite small.

Figures 8 through 10 show how a change in θ_o affects the flutter boundaries. Two values of μ were tested at θ_o = 1 and 3 deg. For μ = 3.19, flutter speeds were higher for larger θ_o; the difference decreased with increasing values of x_α. There was no definite trend in the flutter frequencies. The phase angles were higher at the larger angle of attack and the differences increased with increasing values of

x_α. For $\mu = 2.18$, the flutter boundaries were poorly defined since fewer values of x_α were tested and no flutter-free runs were made below the indicated boundaries at $\theta_o = 1$ deg. Therefore the effect of θ_o on flutter boundaries is not clearly established.

The effect of depth variation on flutter characteristics for two values of μ and two values of θ_o is illustrated in Figures 11 through 16. Increasing the depth of the foil decreased the flutter speed, increased the flutter frequency, and had a mixed effect on phase angle. Depth effects were primarily evident in data for 0.5- and 1-chord depths. In many cases, however, insufficient test runs were made to resolve differences that may have existed between 1- and 1.5-chord depths. Flutter speeds for different depths converged slightly with increasing x_α at $\theta_o = 1$ deg but maintained a nearly constant difference at $\theta_o = 3$ deg.

The 1966 test series was intended to survey the effect of heave frequency f_h on the flutter boundaries by using several coil spring combinations in the foil suspensions. Unfortunately the springs had different masses so that μ and β also varied. Therefore the flutter boundaries obtained cannot be plotted as continuous functions of frequency ratio ω_h/ω_α. Nevertheless, the effect of heave frequency on the flutter boundaries can be seen when the data are plotted as shown in Figures 17 and 18. The experimental points are accompanied by short segments of theoretical curves which show the magnitudes of expected discontinuities. It may be seen that to the extent that μ and β changes were small, flutter speeds and frequencies were slowly varying functions of frequency ratio ω_h/ω_α. Phase angles are not available for this test series because foil motions were recorded at too slow a recording chart speed.

To determine the reproducibility of the observed flutter boundaries, several values of μ, θ_o, and foil depth were repeated in each series of towing basin tests. Flutter points based on these nominally equivalent parameter values are shown in Figures 19 through 21. The agreement of flutter speeds for the three tests was excellent at high values of x_α but deteriorated as x_α decreased. On the other hand, the agreement of flutter frequency ratios was good at low values of x_α but became poor as x_α increased. Phase angle results, available from two of the three towing basin tests, were in approximate agreement. It is apparent that the data from the different tests are not equivalent.

Although all of the test parameters were nominally equivalent in value, it is possible that errors in setting the parameter values for each test resulted in the observed discrepancies. Errors of this type would be most likely to occur in θ_o and the foil depth. Both of these parameters were set and were not changed during any single set of tests. Discrepancies in depth could have resulted only from small variations in water level in the basin. Discrepancies in θ_o could have resulted from experimental uncertainty in setting the angle of the foil. A different kind of error might have been introduced by changes in spring constants of the foil suspension over a period of time. The data obtained from systematic variation of these parameters were reexamined to determine the source of the discrepancies.

The effect of changing zero-speed angle of attack θ_o can be seen in Figure 8a. The spread in flutter speeds which occurred for different values of θ_o decreased with increasing values of x_α until the boundaries intersected at $x_\alpha = 0.534$. The same trend occurred among the flutter data from different test series, suggesting that differences in θ_o may have caused the observed discrepancies. When depth effects are considered, Figures 11a and 11b imply that flutter speeds obtained at different depths would exhibit the same trend but that the spread would not disappear at high x_α for depths shallower than 1 chord. Since flutter speeds from the three towing basin tests were in good agreement at high values of x_α, it appears unlikely that there were substantial variations in foil depth settings. The static spring calibrations, made for the 1964 and 1966 tests, showed a 2-percent variation in ω_h/ω_α, which would be too small to affect the results. It is felt, therefore, that the differences among the test series were due to random variations in zero-speed angle of attack settings.

This conclusion is supported by the relatively close agreement between the 1964 water-tunnel and towing-basin test results, shown in Figures 5 through 7. These results were obtained by transferring the test apparatus from one facility to the other without resetting θ_o. Differences in θ_o of as much as 1 deg would be expected because of the difficulty in setting the angle. The angle was set by replacing the NACA profile hydrofoil with a flat-sided foil and aligning the inner suspension housings

with a gunner's quadrant placed on the flat-sided foil. During the 1965 test, the angle of attack was decreased from 3 to 1 deg, rather than being reset at 1 deg; this change in angle of attack may have been more precise than the independently set initial values.

On the basis of the angle of attack effects illustrated in Figure 8 it is possible to determine the relative angles of attack among the three towing basin tests. Since a larger angle of attack produced a higher flutter speed, it may be seen from Figure 19a that the highest angle of attack occurred in the 1965 test, with successively lower angles of attack in 1966 and 1964. In view of the cavitation on the foil which was observed during the 1966 test series, it is probable that even more extensive cavitation occurred during the 1965 test because of a higher angle of attack and, in some cases, shallower depths. It is perhaps significant in this regard that agreement with the computed inception cavitation number was obtained during the 1964 water tunnel test. This result implies that the foil angle of attack was closer to 3 deg during the 1964 tests than during the later tests.

THEORETICAL FLUTTER ANALYSIS

Theoretical flutter boundaries for the hydrofoil system tested were calculated using Equation [1]. Hydrodynamic load expressions derived by Theodorsen[13] were used to represent the flow around a fully wetted hydrofoil operating in an infinite medium. Potential flow was assumed. The resulting flutter speeds, frequencies, and phase angles are plotted in reduced form along with the data in Figures 5 through 21.

The parameters which were surveyed experimentally in the two test facilities included mass ratio μ, mass unbalance x_α, heave frequency f_h, zero-speed angle of attack θ_0, and foil depth. The following discussion compares the effects of these parameters with theoretical predictions.

Three of the four tests were carried out using three values of mass ratio: 3.19, 2.18, and 1.33. Predicted flutter speeds agreed well with experimental values for $\mu = 3.19$, were unconservative by about 12 percent for $\mu = 2.18$, and were grossly unconservative for $\mu = 1.33$; see Figure 5. Predicted flutter frequencies and phase angles (Figures 6 and 7) similarly displayed a wide variation in agreement with experimental values for the

three mass ratios tested. The dependence of the flutter boundaries on mass unbalance x_α, as measured by the slopes of the theoretical and experimental curves, was predicted fairly well. The data presented in Figures 8 through 21 bear a similar relationship to theoretical predictions in that, regardless of which other parameters were varied, agreement was determined primarily by the value of mass ratio. Again, dependence on x_α was given fairly well by theory.

The fourth flutter test was intended to survey heave stiffness, but the experimental technique introduced changes in μ and δ as well. Nevertheless an indication of the effect of heave stiffness can be obtained from the theoretical curve segments plotted with the data in Figures 17 and 18. It should be noted that theoretical results depend only on the ratio ω_h/ω_α and not on heave frequency, so that ω_h/ω_α was used as the independent parameter in plotting the results. Both theory and experiment showed a gradual decrease in flutter speed as ω_h/ω_α increased, but agreement in magnitude depended on the mass ratio range of the data. The correctness of the flutter frequency predictions also appeared to depend more on mass ratio than on ω_h/ω_α.

Under the conditions of potential flow assumed in the Theodorsen loading theory, all flutter boundaries are predicted to be independent of zero-speed angle of attack θ_o. In contrast, variations in θ_o produced significant changes in experimental flutter speeds, frequencies, and phase angles. This failure of the theory may have been due to viscous flow effects which do not appear in potential flow solutions.

The Theodorsen loading theory further assumes that the hydrofoil is in an infinite medium. As a result, free surface effects could not be calculated by this method. Experimental results indicate that foil depth is an important flutter parameter when the hydrofoil is shallower than 1 chord. A theoretical treatment of hydrodynamic loading which includes free surface effects has been published.[14] This theory could be used to calculate flutter boundaries for comparison with the present data, but the calculation was not made for the present report.

The principal difference between the two test facilities was the acceleration that occurred in the towing basin, although foil depth was

also important at shallow depths. Towing carriage acceleration did not significantly affect the flutter points obtained in this study. Therefore the assumption of constant speed is justified.

It has been mentioned that cavitation was observed along the leading edge of the hydrofoil at speeds of 28 knots and above during the 1966 towing basin test and that cavitation was probably present at lower speeds and shallower depths during the 1965 test. The observed cavities did not exceed 0.2 chords in length. Since the cavitation affected the hydrodynamic loading on the foil, the flutter boundaries were also affected. An exact comparison between theory and experiment would therefore require that the flutter curves already discussed be modified to account for cavitation effects. Steinberg and Karp[15] have given unsteady load coefficients for partially cavitating hydrofoils. This load formulation has been used in flutter calculations by Kaplan[16] and by one of the present authors.[6] As discussed in Reference 6, the published load coefficients[15] do not permit well-defined flutter boundaries to be calculated. Therefore theoretical results for partially cavitating hydrofoils will not be presented. It is felt, however, that on the basis of results given in Reference 6, theoretical flutter boundaries in the parameter range tested change only gradually as a function of cavity length for cavities less than 0.25 chords in length.

In summary, the theoretical predictions correctly described the influence of mass unbalance and frequency ratio on the flutter boundaries. The effects of mass ratio and mean angle of attack were not correctly described. Foil depth was not included in the theoretical formulation but was found to be an important flutter parameter. Pre-run acceleration was not treated theoretically and had little effect on flutter boundaries. Cavitation was not treated theoretically, and its effect on flutter boundaries was not determined.

The results obtained confirm the findings of Henry[8] in that an unconservative trend in flutter speed prediction occurred as the hydrofoil mass ratio decreased. Such results fall into the pattern illustrated in Figure 23. It is apparent that there is a deficiency in the theoretical formulation which is strongly dependent on mass ratio. In view of flutter results obtained by Baird et al.,[3] the theory also fails when used in a

representative section calculation in the low mass ratio range typical of full-scale hydrofoils. The present work, while surveying a number of parameters, did not find that any of them had a strong enough effect on flutter speed boundaries to suggest that mass ratio effects were important only for certain ranges of other parameters. However, the experimental parameter ranges were limited and not necessarily representative of full-scale hydrofoil values.

It is felt that in view of the structural simplicity of the hydrofoil system, the hydrodynamic aspects of the theory are deficient. The flow past the hydrofoil was assumed to be two-dimensional, but photographs showed spanwise variations in cavitation at high speeds.

It is noted for reference that theoretical divergence speeds for the hydrofoil system under consideration are substantially higher than the maximum test speeds attained, and in fact could not be plotted in the flutter speed figures at the present scales. The divergence calculation is discussed in Reference 17.

CONCLUSIONS

Flutter boundaries were obtained for a two-degree-of-freedom hydrofoil in approximately two-dimensional flow in a towing basin and a water tunnel. The parameters surveyed were mass ratio, mass unbalance, heave stiffness, angle of attack, and foil depth. All of these parameters significantly affected the flutter boundaries. In contrast, flutter boundaries were essentially unaffected by which test facility was used; flutter characteristics obtained in the 36-in. water tunnel agreed with those obtained at a depth of 1 chord in the towing basin. Therefore flow acceleration was not important.

Comparisons were made with a two-degree-of-freedom flutter calculation which used Theodorsen hydrodynamics in an infinite fluid. The theory correctly predicted the effects of mass unbalance and heave stiffness. The influence of mass ratio was not correctly described; flutter speeds were predicted unconservatively at low mass ratio. The effect of angle of attack was also inadequately treated by the theory. Although the flutter boundaries were theoretically independent of mean angle of

attack, a significant change in flutter speed occurred when angle of attack was changed. The dependence on angle of attack may have been due to viscous effects or to varying amounts of cavitation.

The theoretical flutter boundaries were calculated for a foil at infinite depth. Experimental results approached the theoretical values more closely as the depth of submergence increased. Therefore the theory may represent the correct limiting case insofar as depth is concerned, although deficiencies obviously exist in other areas.

The failure of the theory to treat mass ratio effects successfully is the most significant result since full-scale flutter characteristics must be predicted at low mass ratio where the theory becomes unconservative. The deficiency in treating mass ratio was the same type of deficiency found by other researchers. None of the other parameters surveyed in the present work had a strong enough effect on flutter speed boundaries to suggest that mass ratio effects were dependent on any of the other parameters.

RECOMMENDATIONS

Methods of hydrofoil flutter prediction range in complexity from the elementary representative section theory[13] to the sophisticated modal analysis-lifting surface theory.[7] Although none of the theories has given consistently good flutter predictions, there is only a small amount of data, especially in the mass ratio range of full-scale hydrofoils, with which to compare the theories. It is recommended that both experimental and theoretical work be done as follows.

1. Theoretical work should be done using the elementary representative section theory. Modifications in the hydrodynamic loading formulation should be made, including variations in lift slope and aerodynamic center values as described by Yates[18] for finite span wings, as well as using measured two-dimensional load coefficients given by Pattison.[19] Depth effects should be treated according to the analysis given in Reference 14. The data of Henry[8] and the present report would provide a means of evaluating the modified theory.

2. Experimental work should be performed to define flutter boundaries in the low mass ratio region. Tests using three-dimensional hydrofoils would permit comparisons to be made with all available theories. The tests should include systematic variation of significant flutter parameters such as mass ratio, sweep, and stiffness.

PERSONNEL AND ACKNOWLEDGMENTS

The experimental program was conducted by Mr. Cieslowski. The data analysis and report were done by Mr. Besch. Design of the experimental apparatus was based on a suggestion made by Dr. Charles J. Henry of the Davidson Laboratory, Stevens Institute of Technology, in a conversation with Dr. David A. Jewell and Mr. H.S. Haller of NSRDC. The assistance of Mr. L. Bruce Moore in carrying out the experimental program is appreciated.

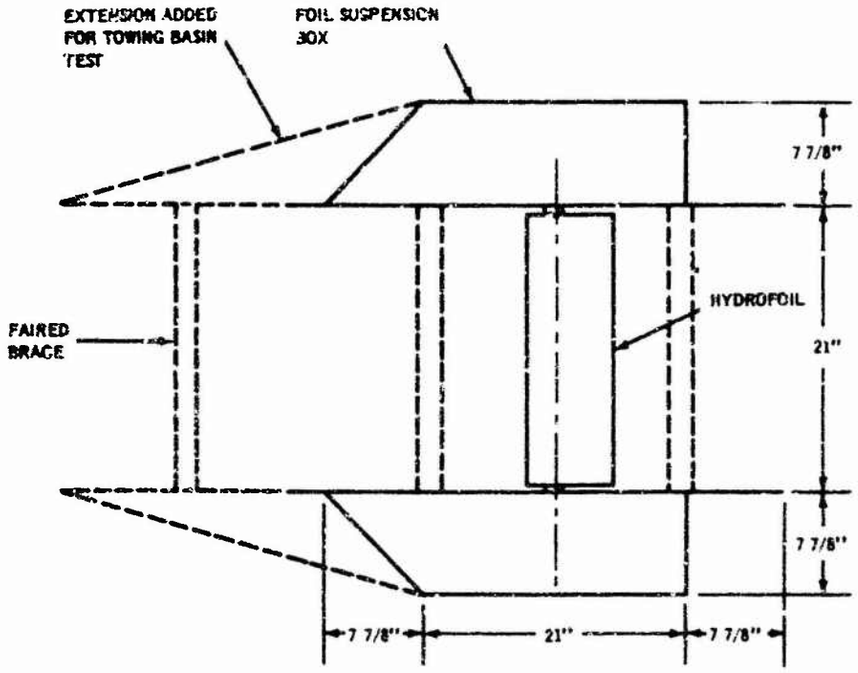

Figure 1a – Top View

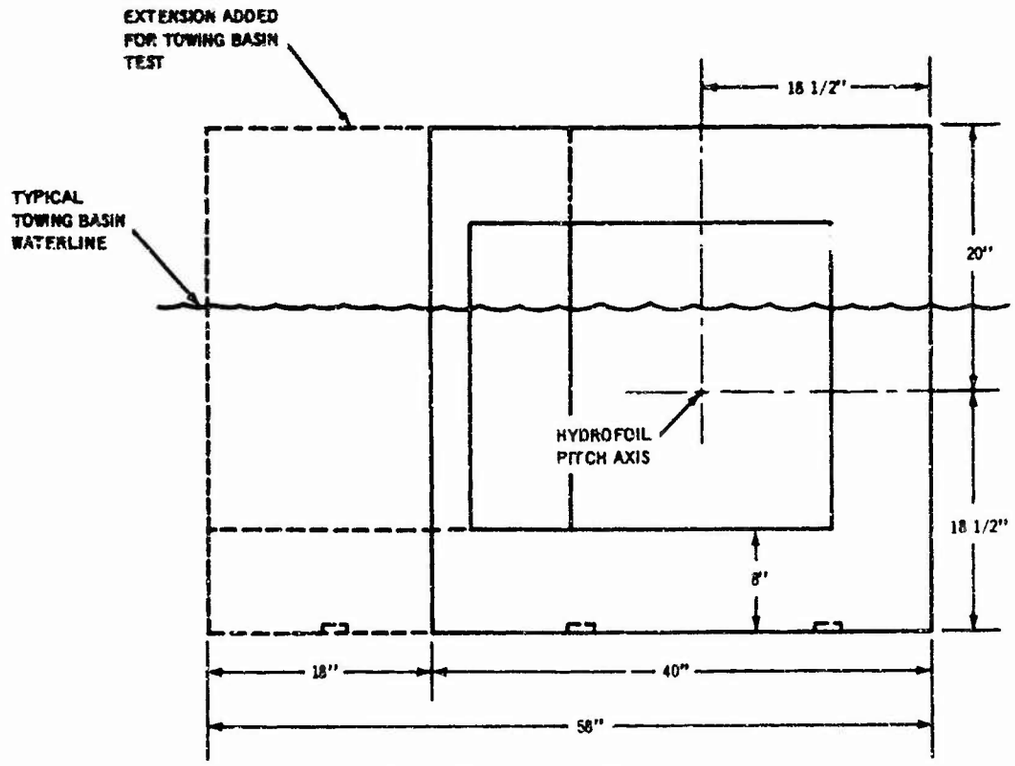

Figure 1b – Port Side View

Figure 1 – Two-Dimensional Test Section

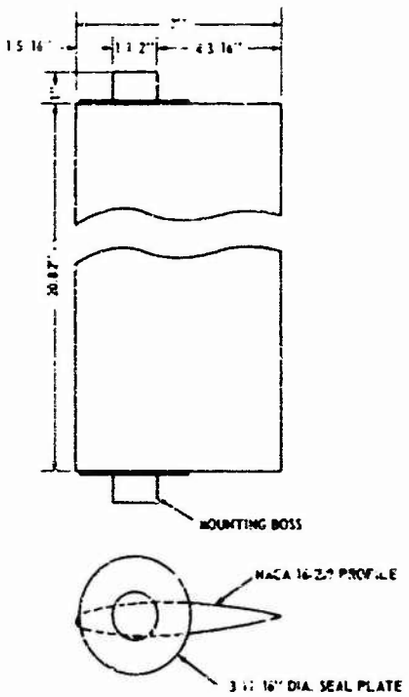

Figure 2 – NACA 16-208
Hydrofoil Model

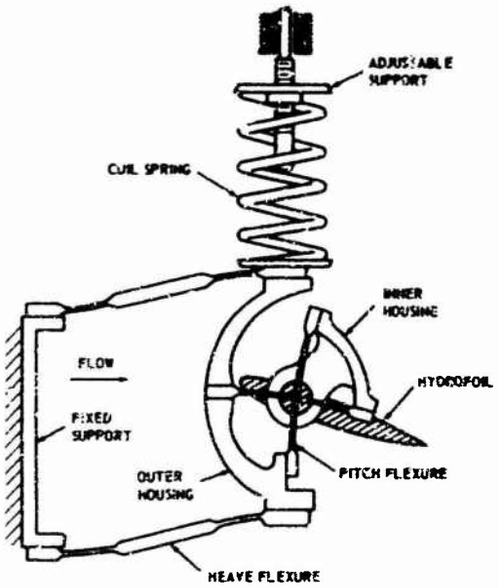

Figure 3 – Two-Degree-of-Freedom
Hydrofoil Suspension

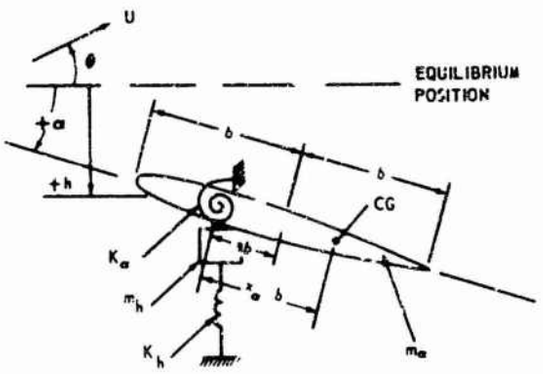

Figure 4 – Hydrofoil System Parameters

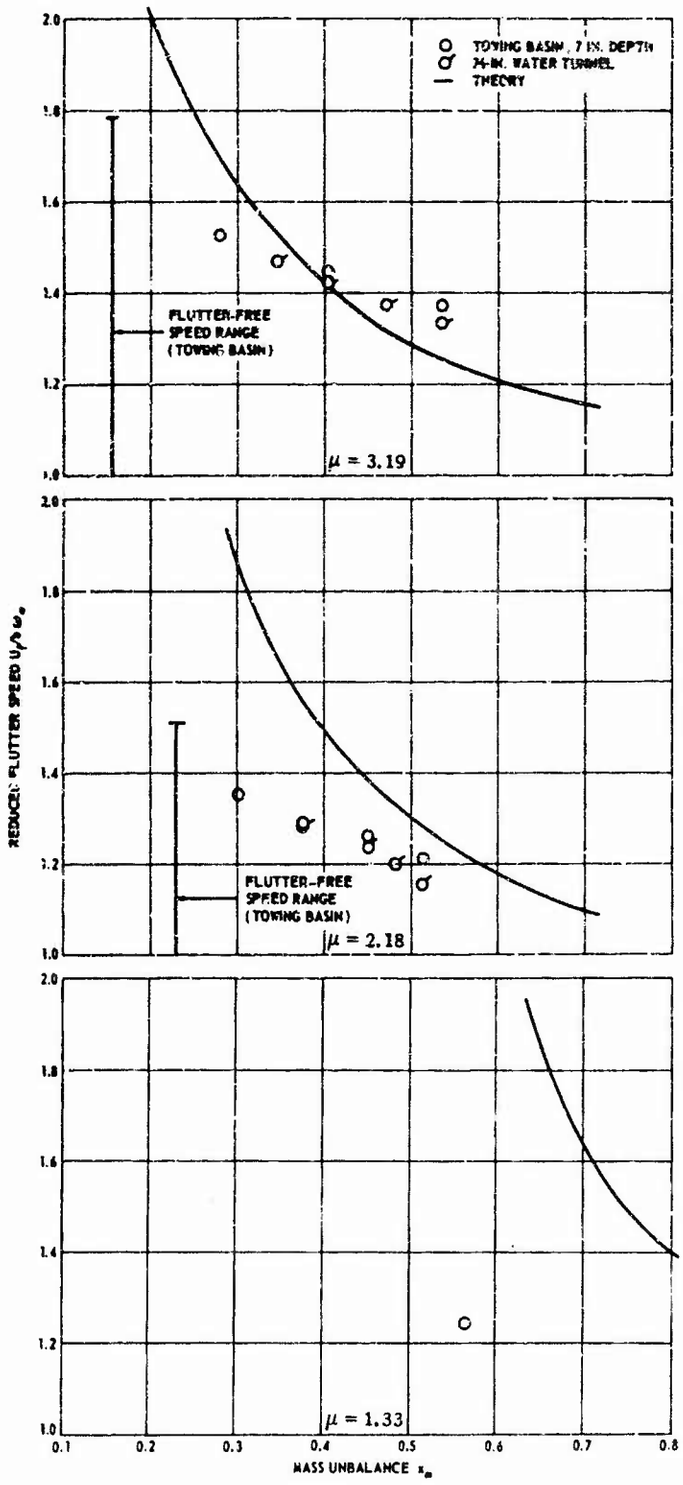

Figure 5 – Reduced Flutter Speed as a Function of Mass Unbalance in the 36-Inch Water Tunnel and in the Towing Basin

θ_0 = 3 deg; foil depth = 7 in. (1 chord); 1964 test data

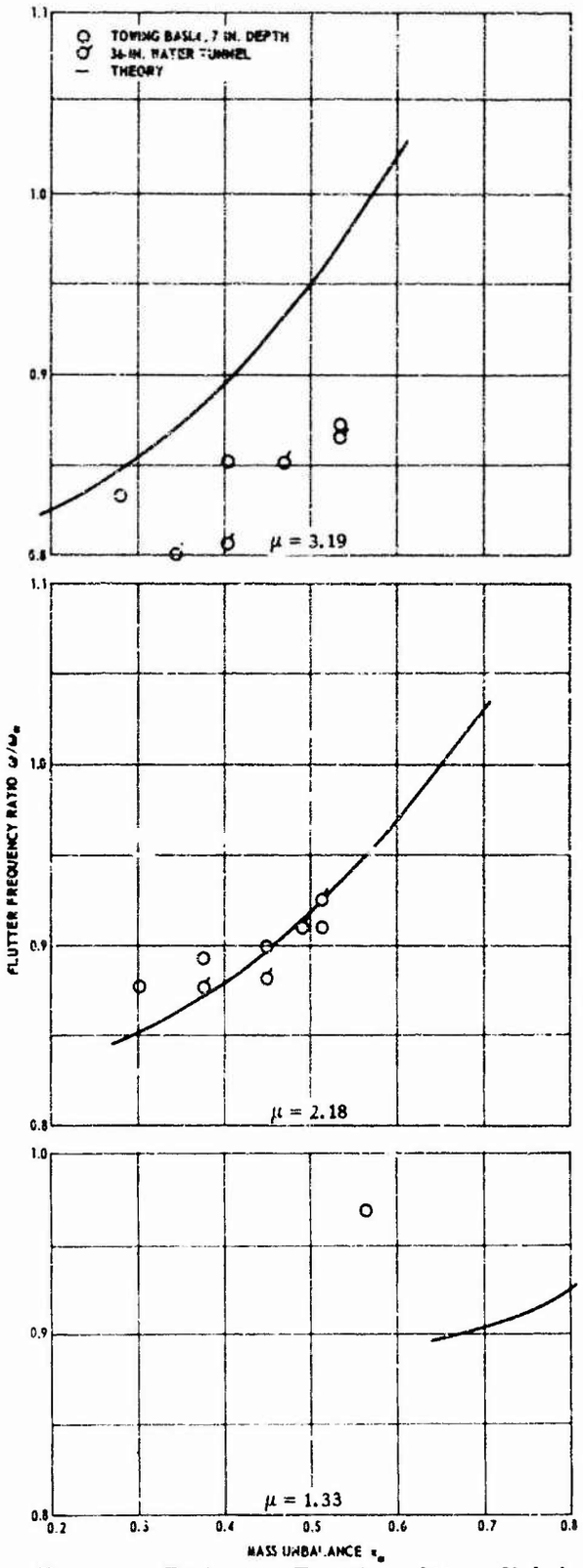

Figure 6 – Flutter Frequency Ratio as a Function of Mass Unbalance in the 36-Inch Water Tunnel and in the Towing Basin

θ_0 = 3 deg; foil depth = 7 in. (1 chord); 1964 test data

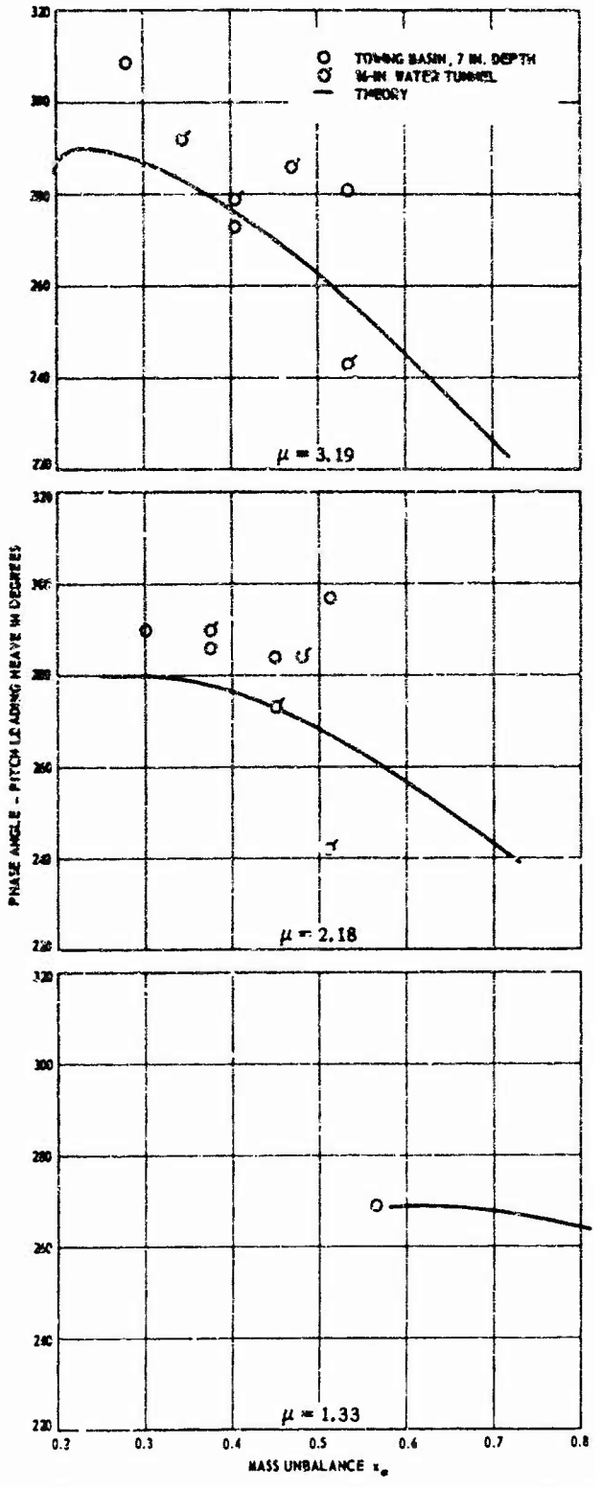

Figure 7 – Relative Phase Angle between Pitch and Heave Motion during Flutter as a Function of Mass Unbalance in the 36-Inch Water Tunnel and in the Towing Basin

θ_0 = 3 deg; foil depth = 7 in. (1 chord); 1964 test data

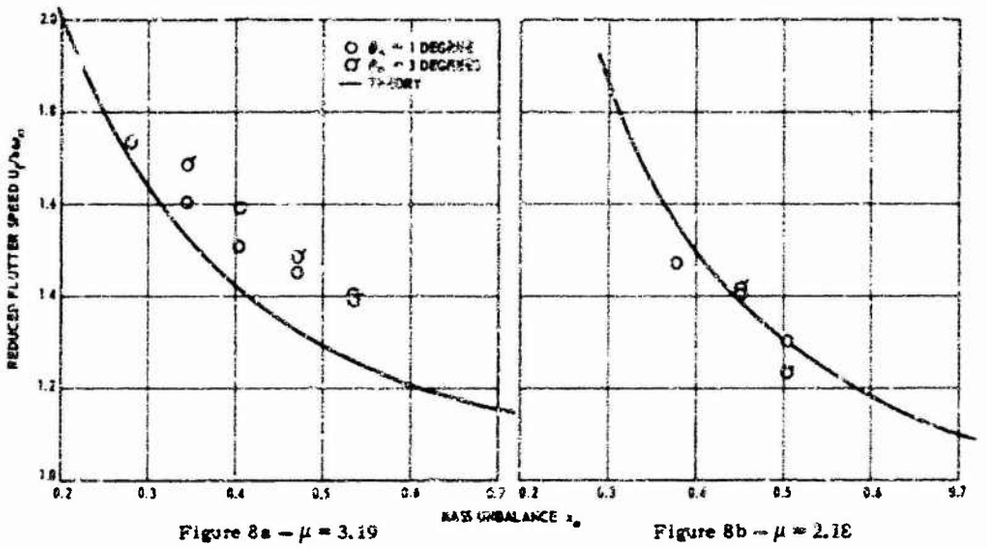

Figure 8a – μ = 3.19 Figure 8b – μ = 2.18

Figure 8 – Reduced Flutter Speed as a Function of Mass Unbalance and Zero-Speed Angle of Attack in the Towing Basin

Foil depth = 7 in. (1 chord); 1965 test data.

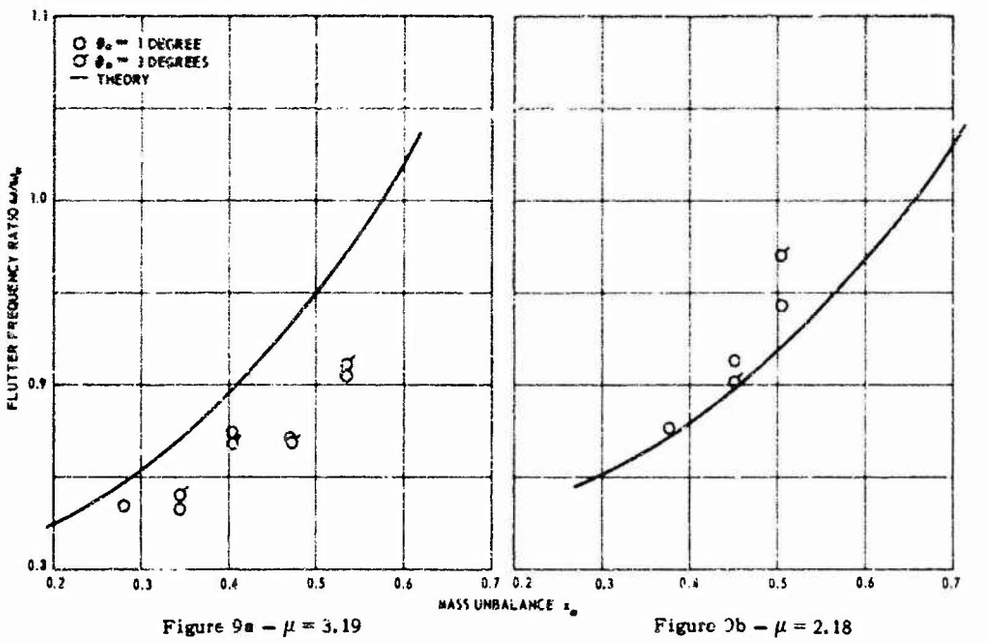

Figure 9a – μ = 3.19 Figure 9b – μ = 2.18

Figure 9 – Flutter Frequency Ratio as a Function of Mass Unbalance and Zero-Speed Angle of Attack in the Towing Basin

Foil depth = 7 in. (1 chord); 1965 test data.

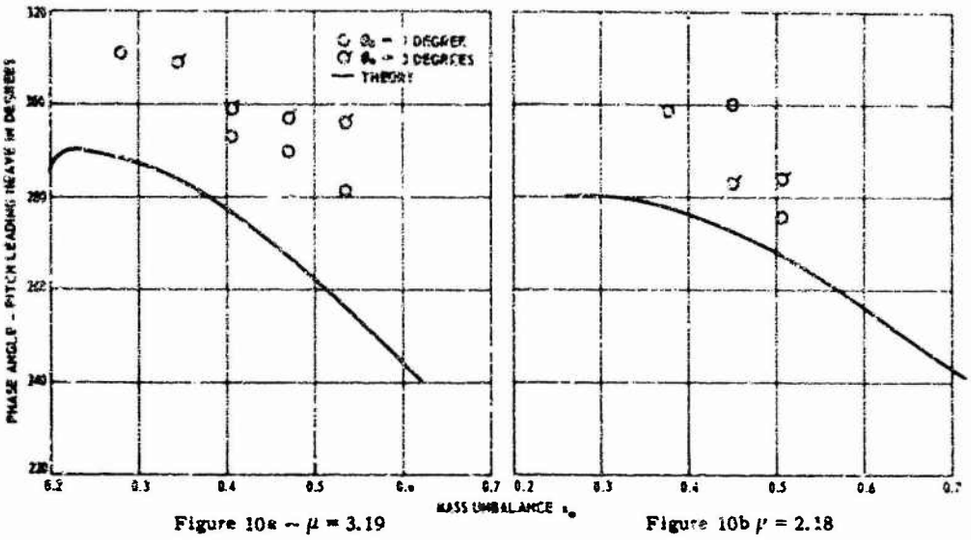

Figure 10a – μ = 3.19 Figure 10b μ = 2.18

Figure 10 – Relative Phase Angle between Pitch and Heave Motion during Flutter as a Function of Mass Unbalance and Zero-Speed Angle of Attack in the Towing Basin

Foil depth = 7 in. (1 chord); 1965 test data.

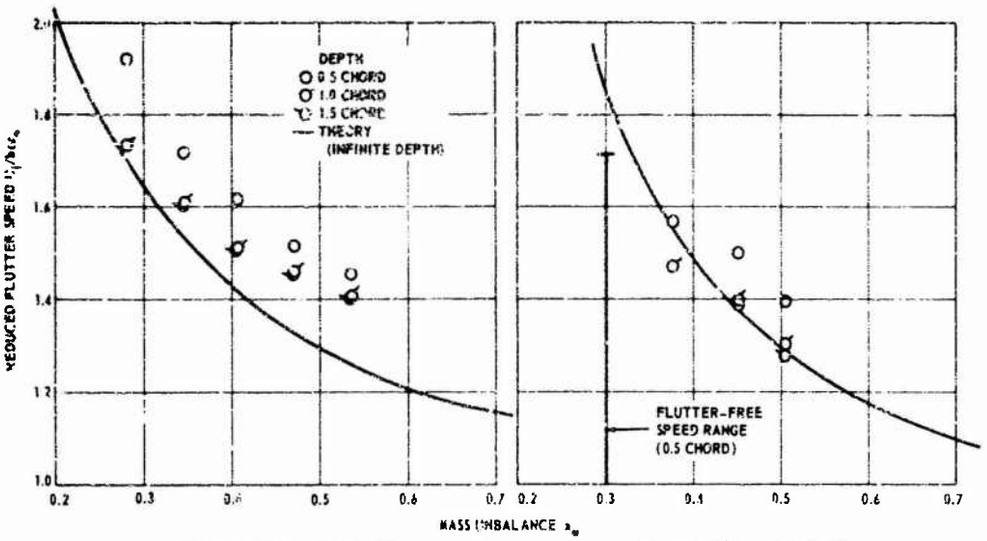

Figure 11a – μ = 3.19 Figure 11b – μ = 2.18

Figure 11 -- Reduced Flutter Speed as a Function of Mass Unbalance and Foil Depth in the Towing Basin

θ_0 = 1 deg; 1965 test data

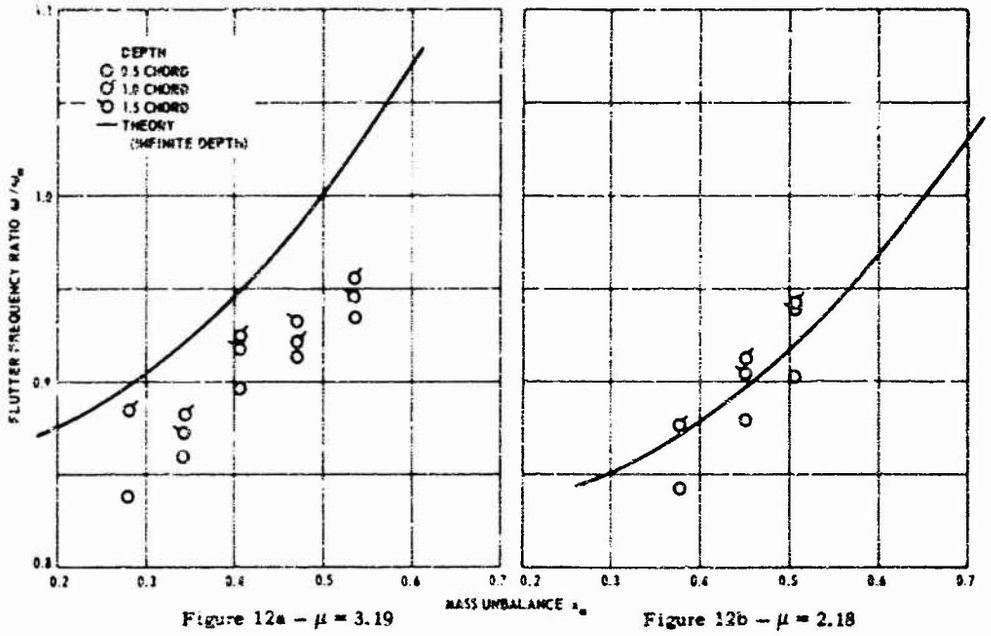

Figure 12a – $\mu = 3.19$

Figure 12b – $\mu = 2.18$

Figure 12 – Flutter Frequency Ratio as a Function of Mass Unbalance and Foil Depth in the Towing Basin

$\theta_0 = 1$ deg; 1965 test data

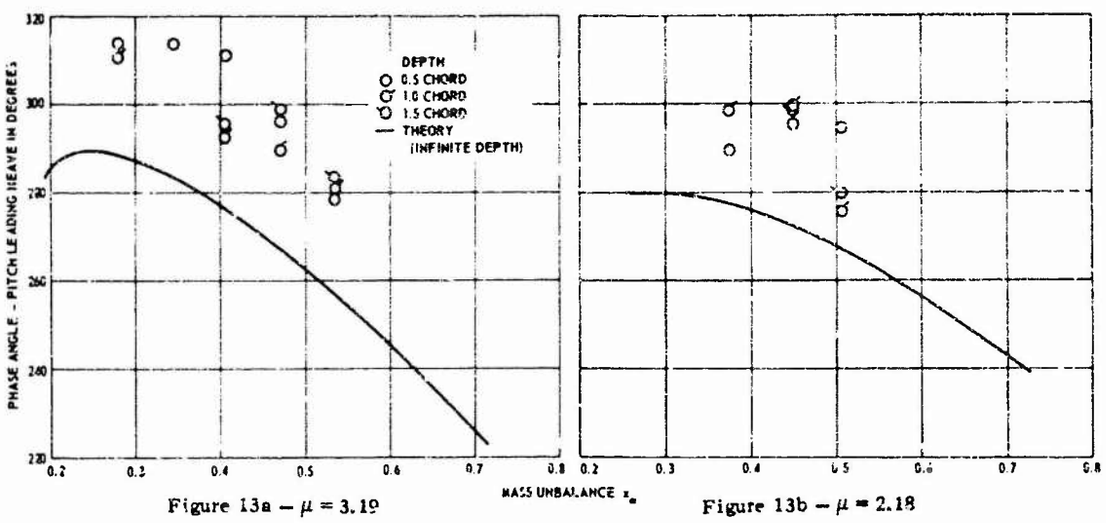

Figure 13a – $\mu = 3.19$

Figure 13b – $\mu = 2.18$

Figure 13 – Relative Phase Angle between Pitch and Heave Motion during Flutter as a Function of Mass Unbalance and Foil Depth in the Towing Basin

$\theta_0 = 1$ deg; 1965 test data

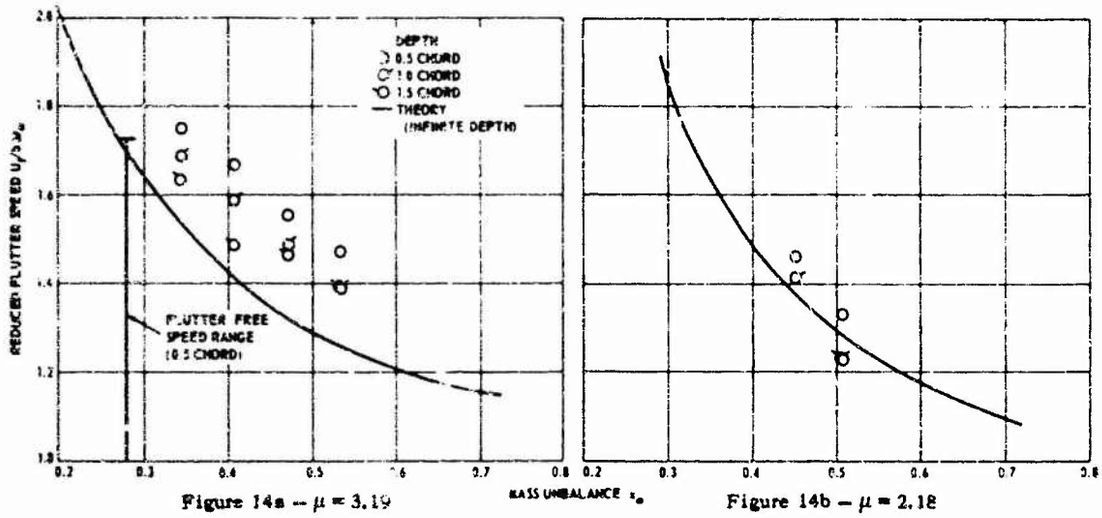

Figure 14a – $\mu = 3.19$ Figure 14b – $\mu = 2.18$

Figure 14 – Reduced Flutter Speed as a Function of Mass Unbalance and Foil Depth in the Towing Basin

$\theta_0 = 3$ deg; 1965 test data

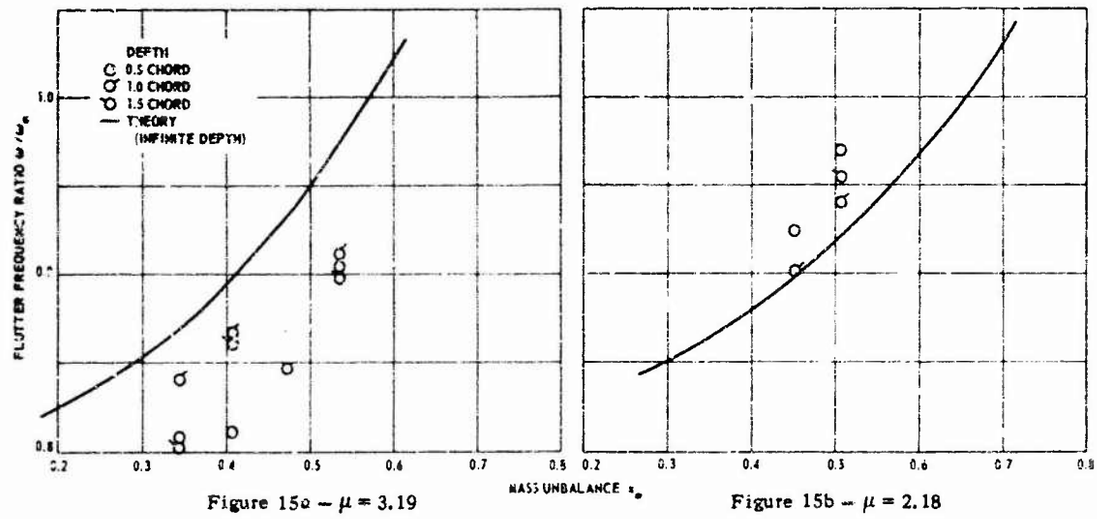

Figure 15a – $\mu = 3.19$ Figure 15b – $\mu = 2.18$

Figure 15 – Flutter Frequency Ratio as a Function of Mass Unbalance and Foil Depth in the Towing Basin

$\theta_0 = 3$ deg; 1965 test data

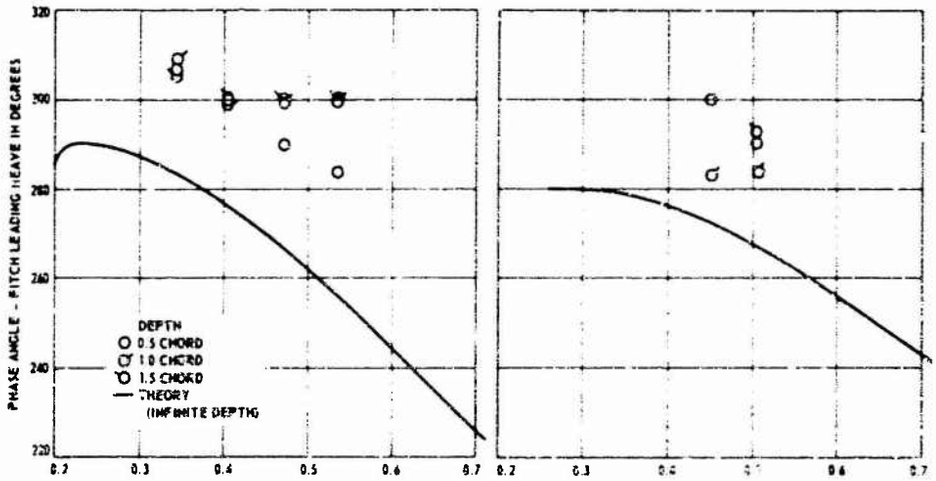

Figure 16a – μ = 3.19

Figure 16b – μ = 2.18

Figure 16 – Relative Phase Angle between Pitch and Heave Motion during Flutter as a Function of Mass Unbalance and Foil Depth in the Towing Basin

θ_0 = 3 deg; 1965 test data

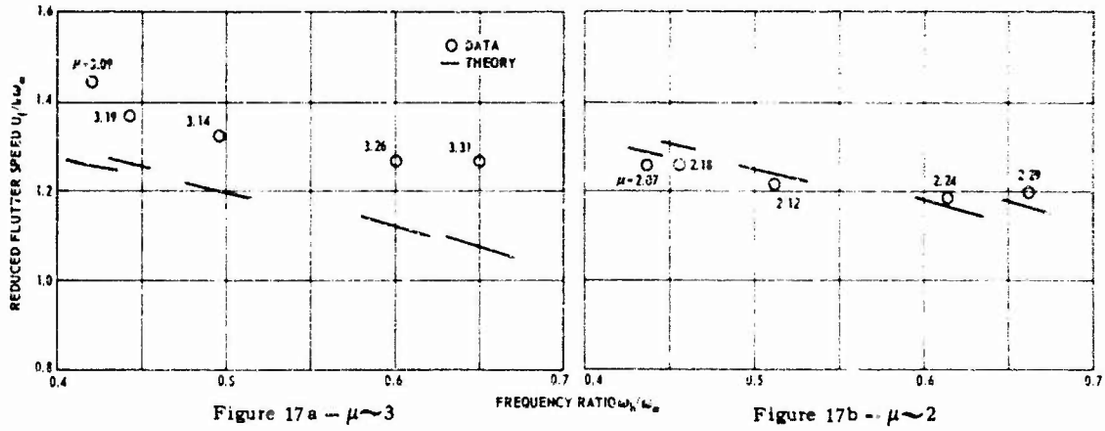

Figure 17a – $\mu \sim 3$

Figure 17b – $\mu \sim 2$

Figure 17 – Reduced Flutter Speed as a Function of Frequency Ratio and Mass Ratio in the Towing Basin

x = 0.534; θ_C = 3 deg; foil depth = 7 in. (1 chord), 1966 test data

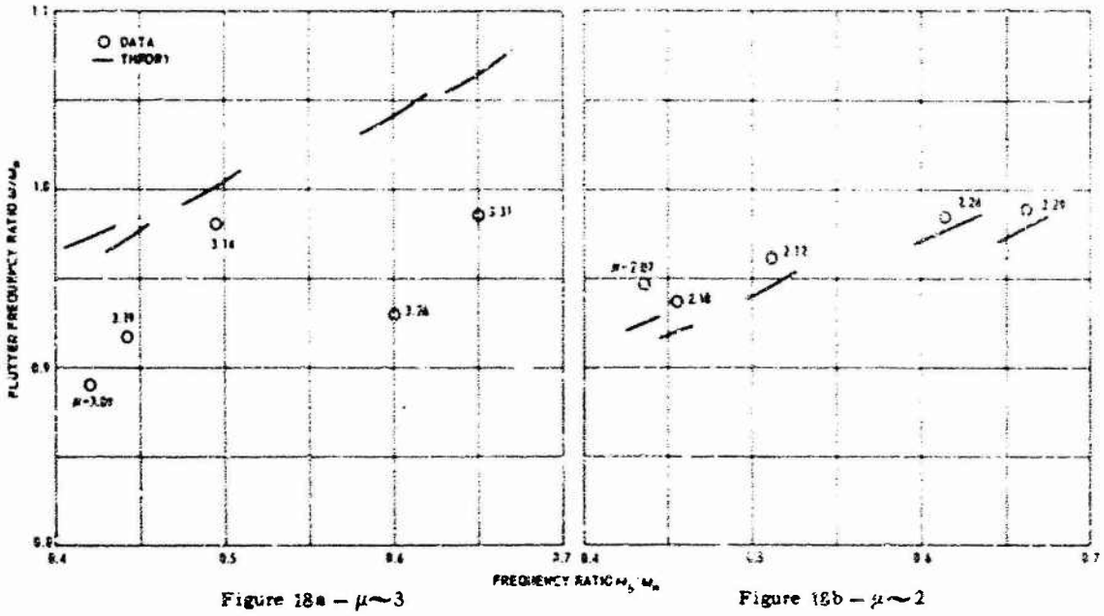

Figure 18a – $\mu \sim 3$ Figure 18b – $\mu \sim 2$

Figure 18 – Flutter Frequency Ratio as a Function of Frequency Ratio and Mass Ratio in the Towing Basin

$x = 0.534$; $\theta_0 = 3$ deg; foil depth = 7 in. (1 chord); 1966 test data

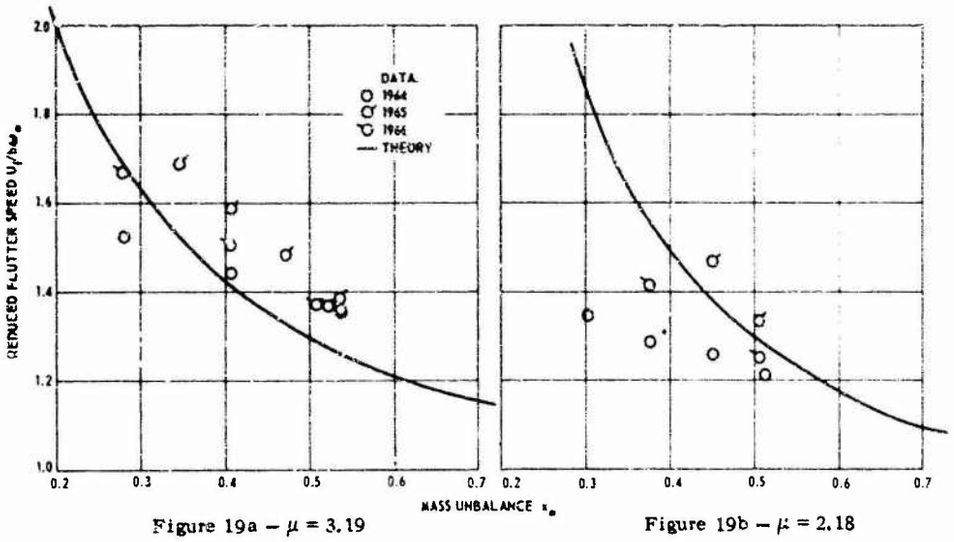

Figure 19a – $\mu = 3.19$ Figure 19b – $\mu = 2.18$

Figure 19 Reduced Flutter Speed as a Function of Mass Unbalance for Three Series of Tests in the Towing Basin

$\theta_0 = 3$ deg; foil depth = 7 in. (1 chord)

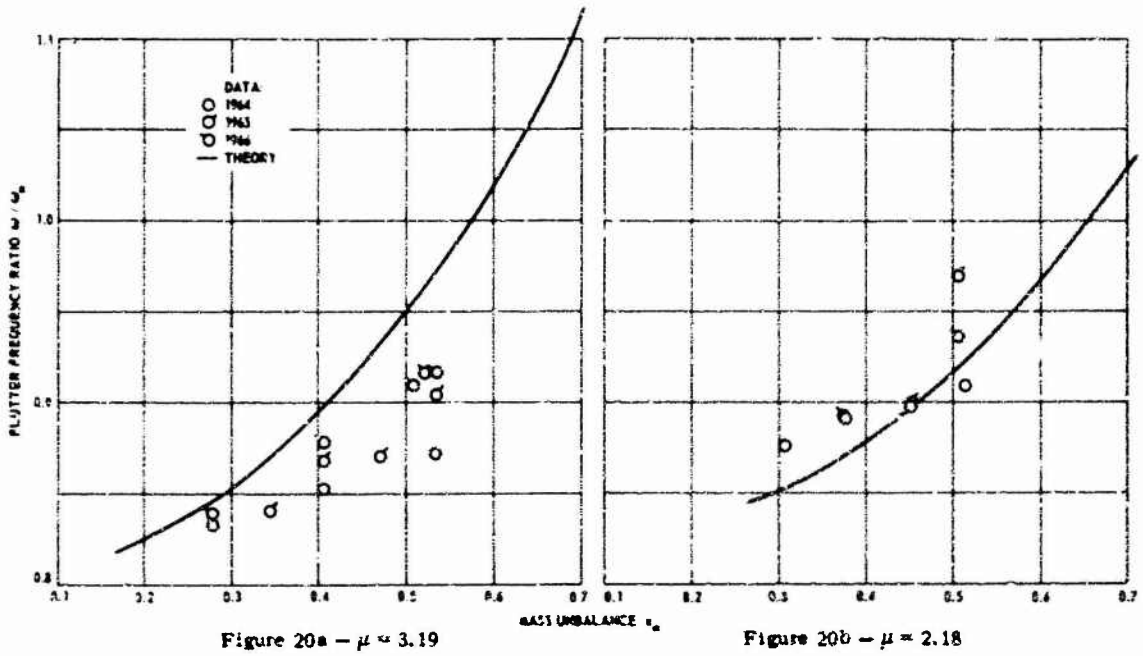

Figure 20a – $\mu = 3.19$ Figure 20b – $\mu = 2.18$

Figure 20 – Flutter Frequency Ratio as a Function of Mass Unbalance for Three Series of Tests in the Towing Basin

$\theta_0 = 3$ deg; foil depth = 7 in. (1 chord)

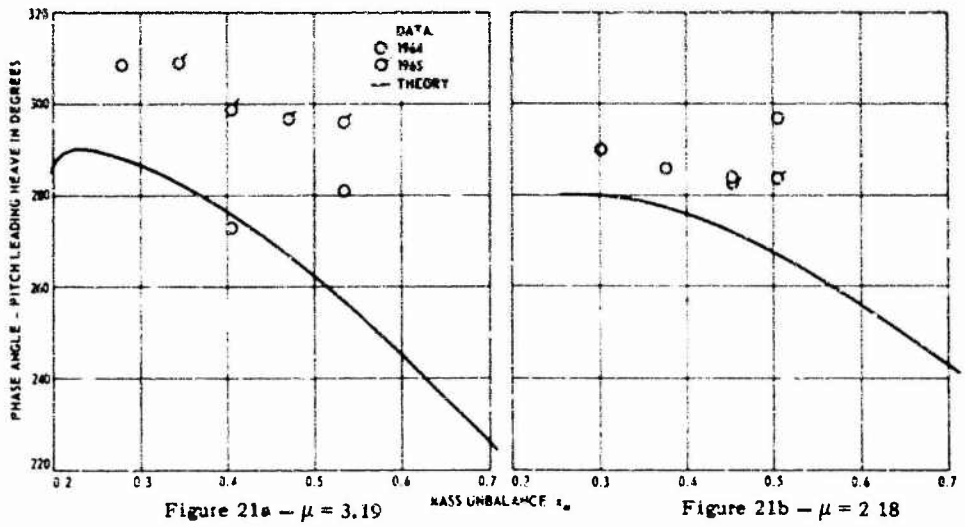

Figure 21a – $\mu = 3.19$ Figure 21b – $\mu = 2.18$

Figure 21 – Relative Phase Angle between Pitch and Heave Motion during Flutter as a Function of Mass Unbalance for Two Series of Tests in the Towing Basin

$\theta_0 = 3$ deg; foil depth = 7 in. (1 chord)

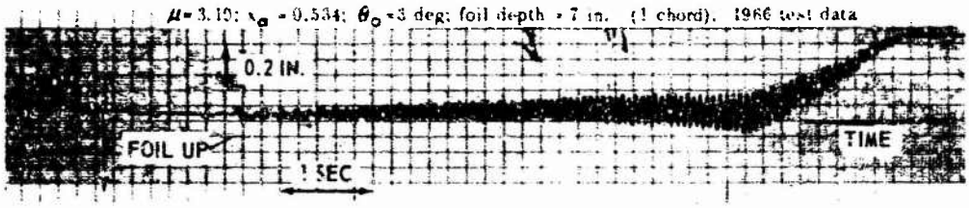

Figure 22a - Pitch Amplitude

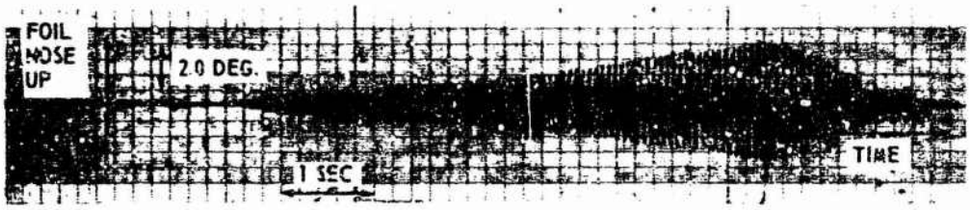

Figure 22b - Pitch Amplitude

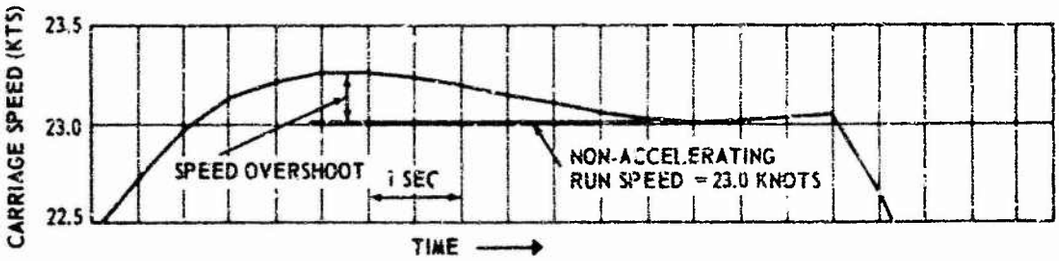

Figure 22c - Carriage Speed

Figure 22 - Oscillograph Records of Heave and Pitch Amplitudes, and a Plot of Carriage Speed, during Flutter in the Towing Basin

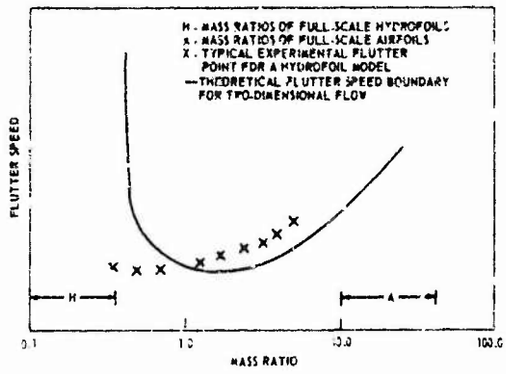

Figure 23 – Relationship between Experimental Flutter Speeds and Theoretical Flutter Speed Boundary as a Function of Mass Ratio

TABLE 1

Structural Parameters of Hydrofoil System as Functions of Mass Ratio

Structural Parameters	Mass Ratios											
	1.33	1.44	2.07	2.12	2.18	2.24	2.29	3.09	3.14	3.19	3.26	3.31
f_h(Hz)	10.62	15.22	7.95	9.32	8.30	11.19	12.08	6.51	7.67	6.85	9.29	10.06
f_α(Hz)	22.82	22.82	18.25	18.25	18.25	18.25	18.25	15.49	15.49	15.49	15.49	15.49
K_h(lb/ft)	5,370	11,976	4,697	6,606	5,370	10,067	11,976	4,697	6,606	5,370	10,067	11,976
r_α	1.262	1.262	1.015	1.015	1.015	1.015	1.015	0.937	0.937	0.937	0.937	0.937
β	0.488	0.449	0.755	0.738	0.719	0.698	0.638	0.825	0.813	0.799	0.763	0.771

Note: Values for other structural parameters were as follows: a = -0.4, b = 0.292 ft, K_α = 1640.9 ft-lb/rad, and s = 1.735 ft.

TABLE 2

Flutter Boundaries Observed during 1964 Flutter Test in 36-Inch Variable-Pressure Water Tunnel

Mass Ratio μ	Mass Unbalance x_α	Flutter Speed U_f knots	Flutter Frequency f_f hertz	Phase Angle degrees
2.18	0.376	25.5	16.0	290
2.18	0.450	24.6	16.1	273
2.18	0.481	23.8	16.6	284
2.18	0.512	22.9	16.9	242
3.19	0.344	24.7	12.4	292
3.19	0.403	24.0	12.5	279
3.19	0.470	23.3	13.2	286
3.19	0.534	22.5	13.4	243

TABLE 3

Flutter Boundaries Observed during 1964 Flutter Test in High-Speed Towing Basin

Mass Ratio μ	Mass Unbalance x_α	Flutter Speed U_f knots	Flutter Frequency f_f hertz	Flutter Free Speed knots	Phase Angle degrees
1.33	0.564	30.8	22.1	--	269
2.18	0.231	--	--	30.0	--
2.18	0.301	26.8	16.0	--	290
2.18	0.376	25.6	16.3	--	286
2.18	0.450	25.0	16.4	--	284
2.18	0.512	24.0	16.6	--	297
3.19	0.155	--	--	30.0	--
3.19	0.279	25.7	12.9	--	309
3.19	0.403	24.3	13.2	--	273
3.19	0.534	23.1	13.5	--	281

TABLE 4

Flutter Boundaries Observed during 1965 Flutter Test in High-Speed Towing Basin at θ_o = 1 Degree

Mass Ratio μ	Mass Unbalance x_α	Hydrofoil Depth inches	Flutter Speed U_f knots	Flutter Frequency f_f hertz	Flutter Free Speed knots	Phase Angle degrees
2.18	0.301	3.5	--	--	34.0	--
2.18	0.376	3.5	31.1	15.4	--	290
2.18	0.376	7.0	29.2	16.0	--	299
2.18	0.450	3.5	29.8	16.1	--	296
2.18	0.450	7.0	27.8	16.7	--	300
2.18	0.450	10.5	27.6	16.5	--	299
2.18	0.503	3.5	27.7	16.7	--	295
2.18	0.503	7.0	25.8	17.2	--	276
2.18	0.503	10.5	25.4	17.1	--	280
3.19	0.279	3.5	32.3	12.2	--	314
3.19	0.279	7.0	29.2	12.9	--	311
3.19	0.344	3.5	28.9	12.6	--	314
3.19	0.344	7.0	27.0	12.9	--	*
3.19	0.344	10.5	27.0	12.8	--	*
3.19	0.403	3.5	27.1	13.1	--	311
3.19	0.403	7.0	25.4	13.6	--	293
3.19	0.403	10.5	25.3	13.5	--	296
3.19	0.470	3.5	25.5	13.4	--	297
3.19	0.470	7.0	24.5	13.5	--	290
3.19	0.470	10.5	24.5	13.7	--	299
3.19	0.534	3.5	24.4	13.7	--	279
3.19	0.534	7.0	23.6	14.0	--	281
3.19	0.534	10.5	23.5	13.9	--	283

*Not available.

TABLE 5

Flutter Boundaries Observed during 1965 Flutter Test in High-Speed Towing Basin at θ = 3 Degrees

Mass Ratio μ	Mass Unbalance x_α	Hydrofoil Depth inches	Flutter Speed U_f knots	Flutter Frequency f_f hertz	Flutter Free Speed knots	Phase Angle degrees
2.18	0.450	3.5	29.1	16.9	--	300
2.18	0.450	7.0	28.1	16.5	--	283
2.18	0.503	3.5	26.5	17.2	--	291
2.18	0.503	7.0	24.5	17.7	--	284
2.18	0.503	10.5	24.5	17.4	--	293
3.19	0.279	3.5	--	--	29.0	--
3.19	0.344	3.5	29.5	12.5	--	309
3.19	0.344	7.0	28.4	13.0	--	309
3.19	0.344	10.5	27.5	12.4	--	296
3.19	0.403	3.5	28.1	12.6	--	300
3.19	0.403	7.0	26.8	13.4	--	299
3.19	0.403	10.5	26.6	13.4	--	300
3.19	0.470	3.5	26.2	13.1	--	290
3.19	0.470	7.0	25.0	13.5	--	297
3.19	0.470	10.5	24.7	13.4	--	297
3.19	0.534	3.5	24.8	14.0	--	284
3.19	0.534	7.0	23.4	14.1	--	296
3.19	0.534	10.5	23.4	13.9	--	295

TABLE 6

Flutter Boundaries Observed during 1966 Flutter Test in High Speed Towing Basin

θ_o = 3 deg and foil depth = 7 in. (1 chord)

Mass Ratio μ	Mass Unbalance x_α	Heave Frequency f_h hertz	Flutter Speed U_f knots	Flutter Frequency f_f hertz	Flutter Free Speed knots
1.44	0.667	15.22	--	--	32.0
2.07	0.376	7.95	28.1	16.4	--
2.07	0.503	7.95	24.9	17.3	--
2.12	0.228	9.32	--	--	30.1
2.12	0.376	9.32	26.3	17.0	--
2.12	0.503	9.32	24.0	17.6	--
2.18	0.376	8.30	28.1	16.3	--
2.18	0.503	8.30	24.9	17.1	--
2.24	0.376	11.19	26.4	17.2	--
2.24	0.503	11.19	23.5	18.0	--
2.29	0.228	12.08	--	--	29.9
2.29	0.376	12.08	26.0	17.3	--
2.29	0.503	12.08	23.7	18.05	--
3.09	0.279	6.51	28.6	12.8	--
3.09	0.403	6.51	24.5	13.5	--
3.09	0.523	6.51	22.2	14.5	--
3.09	0.534	6.51	24.3	13.8	--
3.14	0.279	7.67	27.2	13.2	--
3.14	0.403	7.67	24.2	13.6	--
3.14	0.523	7.67	22.1	14.8	--
3.14	0.534	7.67	22.3	15.2	--
3.19	0.279	6.85	28.2	13.0	--
3.19	0.403	6.85	25.3	13.6	--
3.19	0.506	6.85	23.1	14.1	--
3.19	0.523	6.85	23.0	14.2	--
3.19	0.534	6.85	23.0	14.2	--
3.26	0.279	9.29	26.6	13.6	--
3.26	0.403	9.29	22.5	14.5	--
3.26	0.523	9.29	21.4	15.2	--
3.26	9.534	9.29	21.3	15.0	--
3.31	0.156	10.06	30.1	13.8	--
3.31	0.279	10.06	25.5	13.8	--
3.31	0.403	10.06	21.6	14.6	--
3.31	0.523	10.06	20.6	15.5	--
3.31	0.534	10.06	21.3	15.3	--

REFERENCES

1. Hilborne, D.V., "The Hydroelastic Stability of Struts," Admiralty Research Laboratory Report ARL/R1/G/HY/5/3, Teddington, Middlesex, England (Nov 1958).

2. Jewell, D.A. and McCormick, M.E., "Hydroelastic Instability of a Control Surface," David Taylor Model Basin Report 1442 (Dec 1961).

3. Baird, E.F. et al., "An Experimental and Theoretical Investigation of Hydrofoil Flutter," Aerospace Engineering, Vol. 21, No. 2, pp. 34-41 (Feb 1962).

4. Abramson, H.N. and Ransleben, G.E., Jr., "An Experimental Investigation of Flutter of a Fully Submerged Subcavitating Hydrofoil," Southwest Research Institute, Contract Nonr-3335(00) (Dec 1963).

5. Theodorsen, T. and Garrick, J.E., "Mechanism of Flutter: A Theoretical and Experimental Investigation of the Flutter Problem," NACA Report 685 (1940).

6. Besch, P.K., "Flutter and Cavity-Induced Oscillation of a Two-Degree-of-Freedom Hydrofoil in a Two-Dimensional Cavitating Flow," Naval Ship Research and Development Center Report 3000 (Feb 1969).

7. Rowe, W.S. and Marvin, T.B.G., "A Program of Theoretical Research on Hydroelastic Stability," The Boeing Company, Contract N00014-67-C-0248 (Aug 1968).

8. Henry, C.J., "Comparison of Hydrofoil Flutter Phenomenon and Airfoil Flutter Theory," Proceedings 4th Naval Hydrodynamics Symposium (Aug 1962).

9. Cieslowski, D.S. and Pattison, J.H., "Unsteady Hydrodynamic Loads and Flutter of Two-Dimensional Hydrofoils," Spring Meeting Hydrofoil Symposium, Society of Naval Architects and Marine Engineers, Paper 2-b (May 1965).

10. Brownell, W.F. and Miller, M.L., "Hydromechanics Cavitation Research Facilities and Techniques in Use at the David Taylor Model Basin," Symposium on Cavitation Research Facilities and Techniques, American Society of Mechanical Engineers (May 1964). Also David Taylor Model Basin Report 1856 (Oct 1964).

11. Breslin, J.P. and Landweber, L., "A Manual for Calculation of Inception of Cavitation on Two and Three Dimensional Forms," SNAME Technical and Research Bulletin 1-21 (Oct 1961).

12. Macovsky, M.S. et al., "Predicted Cavitation Characteristics for the TMB-EPH Strut Section Compared with Those for the Bureau of Ships Standard Strut Section," David Taylor Model Basin Report 879 (Jan 1948).

13. Bisplinghoff, R.L. et al., "Aeroelasticity," Addison-Wesley Publishing Company, Cambridge, Massachusetts (1955), pp. 251-281.

14. Ashley, H. et al., "New Directions in Lifting Surface Theory," AIAA Journal, Vol. 3, No. 1, pp. 3-16 (1965).

15 Steinberg, H. and Karp, S., "Unsteady Flow Past Partially Cavitated Hydrofoils," Proceedings 4th Naval Hydrodynamics Symposium (Aug 1962).

16. Kaplan, P., "Hydroelastic Instabilities of Partially Cavitated Hydrofoils," Proceedings 4th Naval Hydrodynamics Symposium (Aug 1962).

17. Abramson, H.N. et al., "Hydroelasticity with Special Reference to Hydrofoil Craft," NSRDC Report 2557, pp. 423-435 (Sep 1967).

18. Yates, E.C., Jr., "Calculation of Flutter Characteristics for Finite-Span Swept or Unswept Wings at Subsonic and Supersonic Speeds by a Modified Strip Analysis," NACA RM L57L10 (1958).

19. Pattison, John H., "Hydrodynamic Loads on a Two-Dimensional Hydrofoil," NSRDC Report 3245 (in preparation).

UNCLASSIFIED

Security Classification

DOCUMENT CONTROL DATA - R & D

(Security classification of title, body of abstract and indexing annotation must be entered when the overall report is classified)

1. ORIGINATING ACTIVITY (Corporate author) Naval Ship Research & Development Center Washington, D.C. 20007	2a. REPORT SECURITY CLASSIFICATION UNCLASSIFIED 2b. GROUP

3. REPORT TITLE

FLUTTER OF A TWO-DEGREE-OF-FREEDOM HYDROFOIL IN TWO-DIMENSIONAL SURCAVITATING FLOW

4. DESCRIPTIVE NOTES (Type of report and inclusive dates)

Final Report

5. AUTHOR(S) (First name, middle initial, last name)

Daniel S. Cieslowski and Peter K. Besch

6. REPORT DATE	7a. TOTAL NO. OF PAGES	7b. NO. OF REFS
January 1970	46	19

8a. CONTRACT OR GRANT NO.	9a. ORIGINATOR'S REPORT NUMBER(S)
b. PROJECT NO. Subproject No. S4606 Task 1703	3183 9b. OTHER REPORT NO(S) (Any other numbers that may be assigned this report)

10. DISTRIBUTION STATEMENT

This document has been approved for public release and sale; its distribution is unlimited.

11. SUPPLEMENTARY NOTES	12. SPONSORING MILITARY ACTIVITY
	Naval Ship Systems Command

13. ABSTRACT

Four hydrofoil flutter tests were performed in the towing basin and the 36-inch water tunnel at the Naval Ship Research and Development Center using a two-degree-of-freedom hydrofoil in two-dimensional flow. Mass ratio, mass unbalance, heave stiffness, angle of attack, and foil depth were varied. All of these parameters significantly affected the flutter boundaries.

Comparisons were made with a flutter theory based on the Theodorsen analysis. Theory gave good flutter predictions at high mass ratios but failed at low mass ratios.

DD FORM 1 NOV 68 1473 (PAGE 1)

S/N 0101-807-6801

UNCLASSIFIED

Security Classification

14 KEY WORDS	LINK A		LINK B		LINK C	
	ROLE	WT	ROLE	WT	ROLE	WT
Flutter						
Towing Basin Testing						
Water Tunnel Testing						
Theodorsen Flutter Theory						